

Summary

- Subject ID: 09
- Structural images: 1 T1-weighted
- Functional series: 1
 - Task: rhymejudgment (1 run)
- Standard output spaces: MNI152NLin2009cAsym, fsaverage5, MNI152NLin6Asym
- Non-standard output spaces: anat, fsnative
- FreeSurfer reconstruction: Run by fMRIPrep

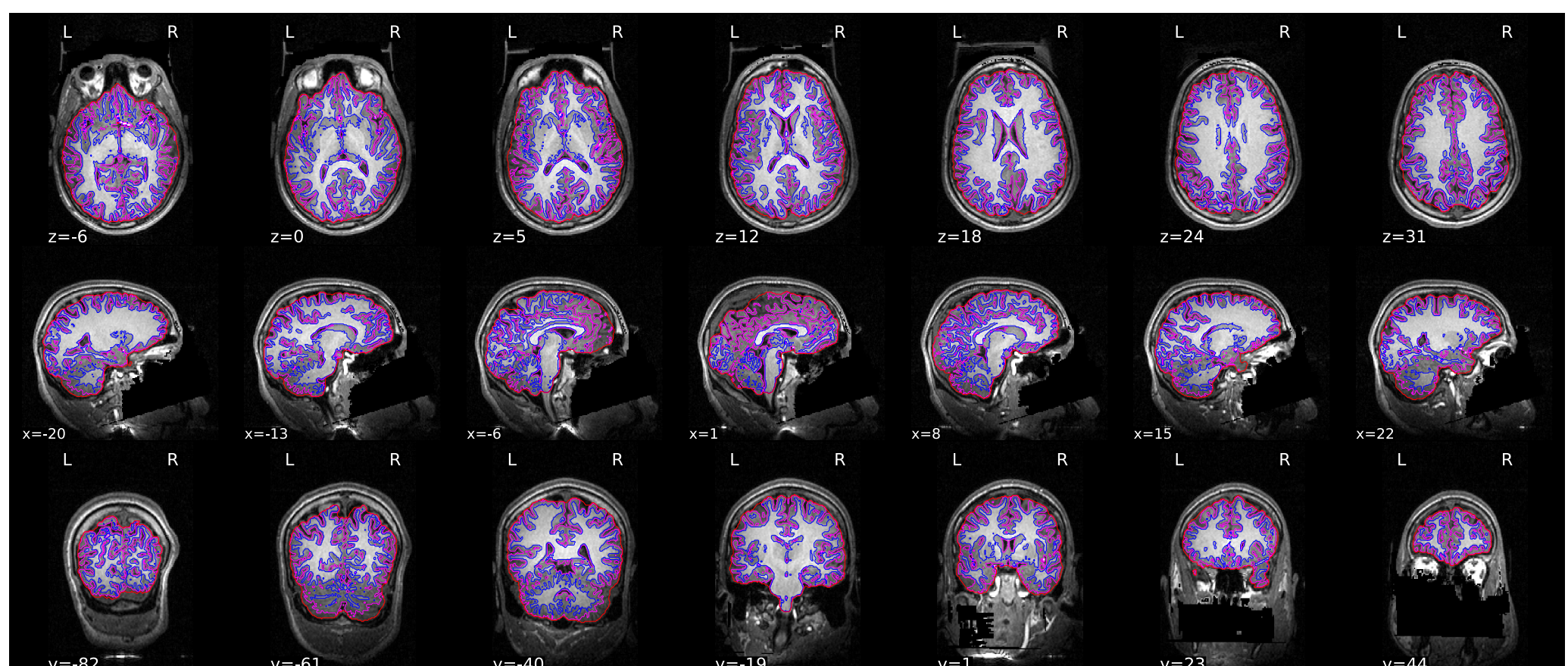
Anatomical

Anatomical Conformation

- Input T1w images: 1
- Output orientation: RAS
- Output dimensions: 160x192x192
- Output voxel size: 1mm x 1.3mm x 1.3mm
- Discarded images: 0

Brain mask and brain tissue segmentation of the T1w

This panel shows the template T1-weighted image (if several T1w images were found), with contours delineating the detected brain mask and brain tissue segmentations.

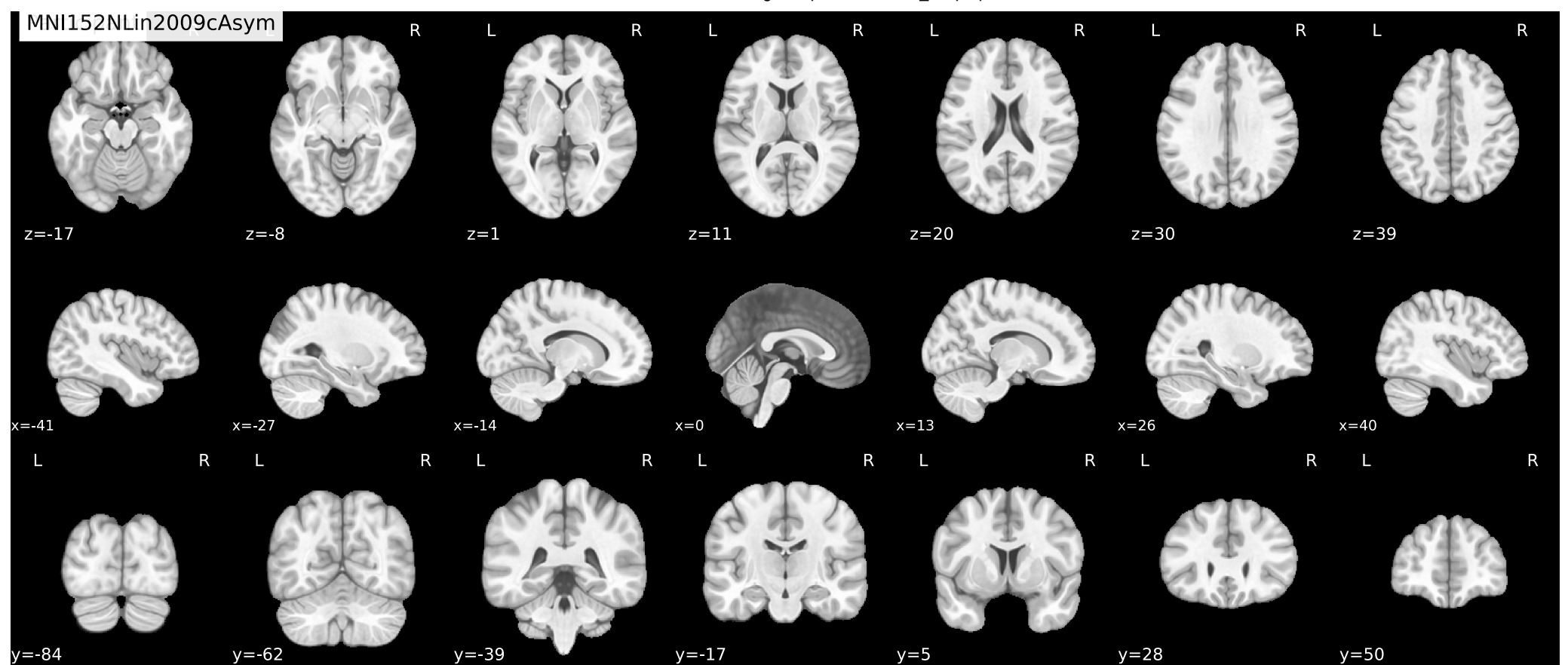


Get figure file: [sub-09/figures/sub-09_dseg.svg](#)

Spatial normalization of the anatomical T1w reference

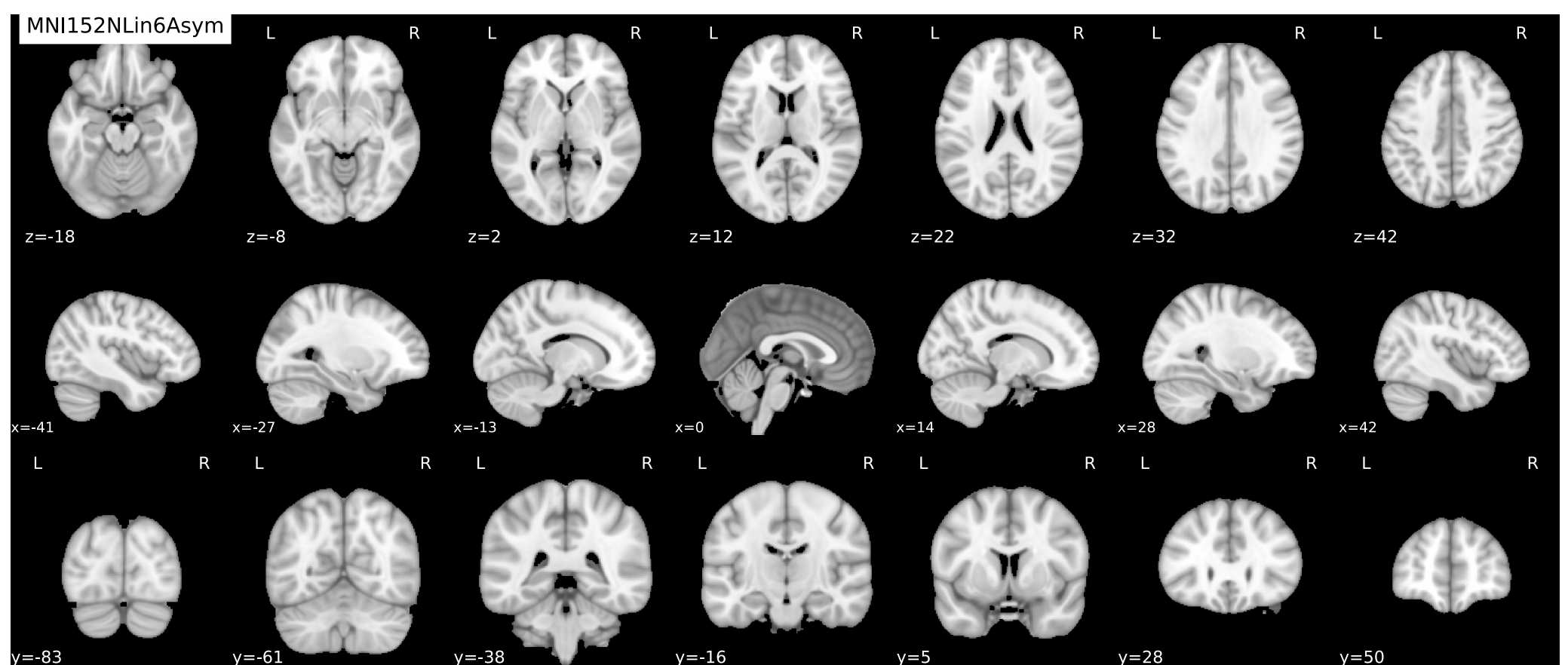
Results of nonlinear alignment of the T1w reference one or more template space(s). Hover on the panels with the mouse pointer to transition between both spaces.

Spatial normalization of the T1w image to the [MNI152NLin2009cAsym](#) template.



Get figure file: [sub-09/figures/sub-09_space-MNI152NLin2009cAsym_T1w.svg](#)

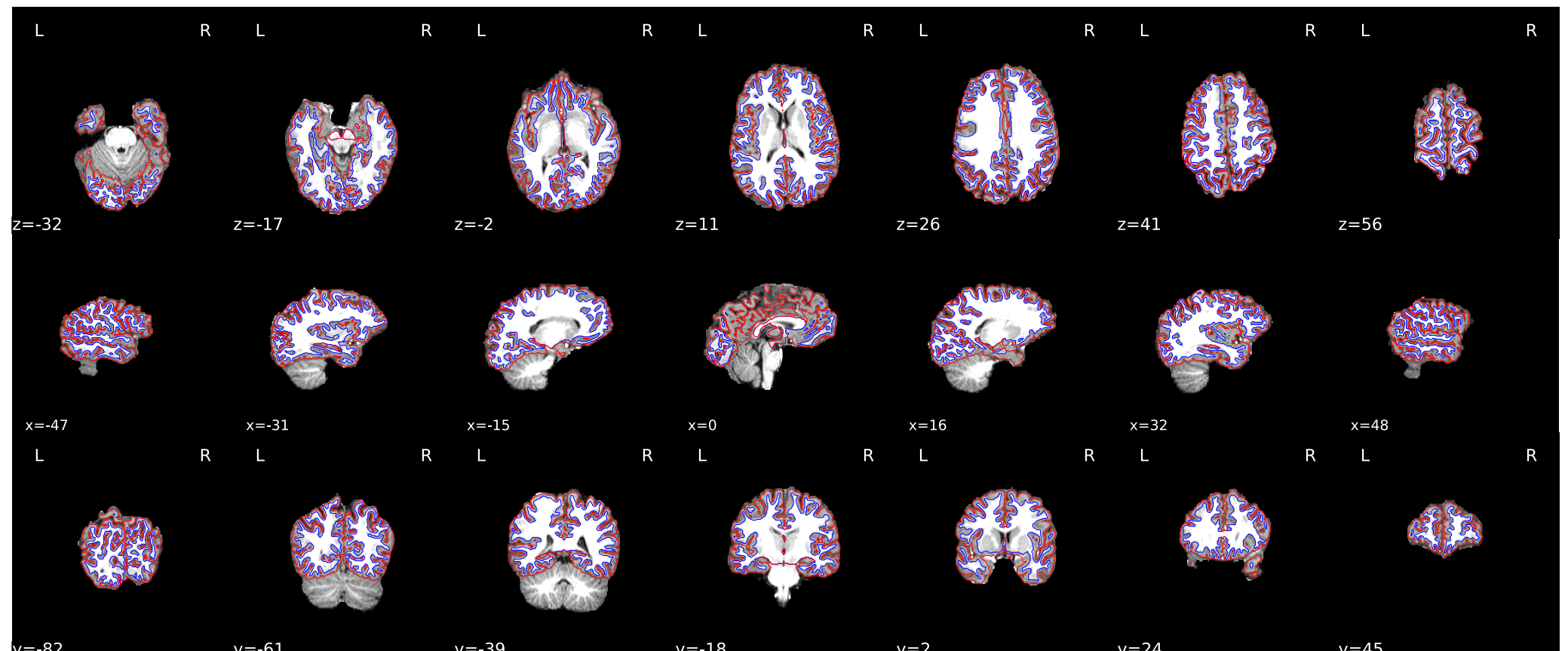
Spatial normalization of the T1w image to the **MNI152NLin6Asym** template.



Get figure file: [sub-09/figures/sub-09_space-MNI152NLin6Asym_T1w.svg](#)

Surface reconstruction

Surfaces (white and pial) reconstructed with FreeSurfer (`recon-all`) overlaid on the participant's T1w template.



Get figure file: [sub-09/figures/sub-09_desc-reconall_T1w.svg](#)

Functional

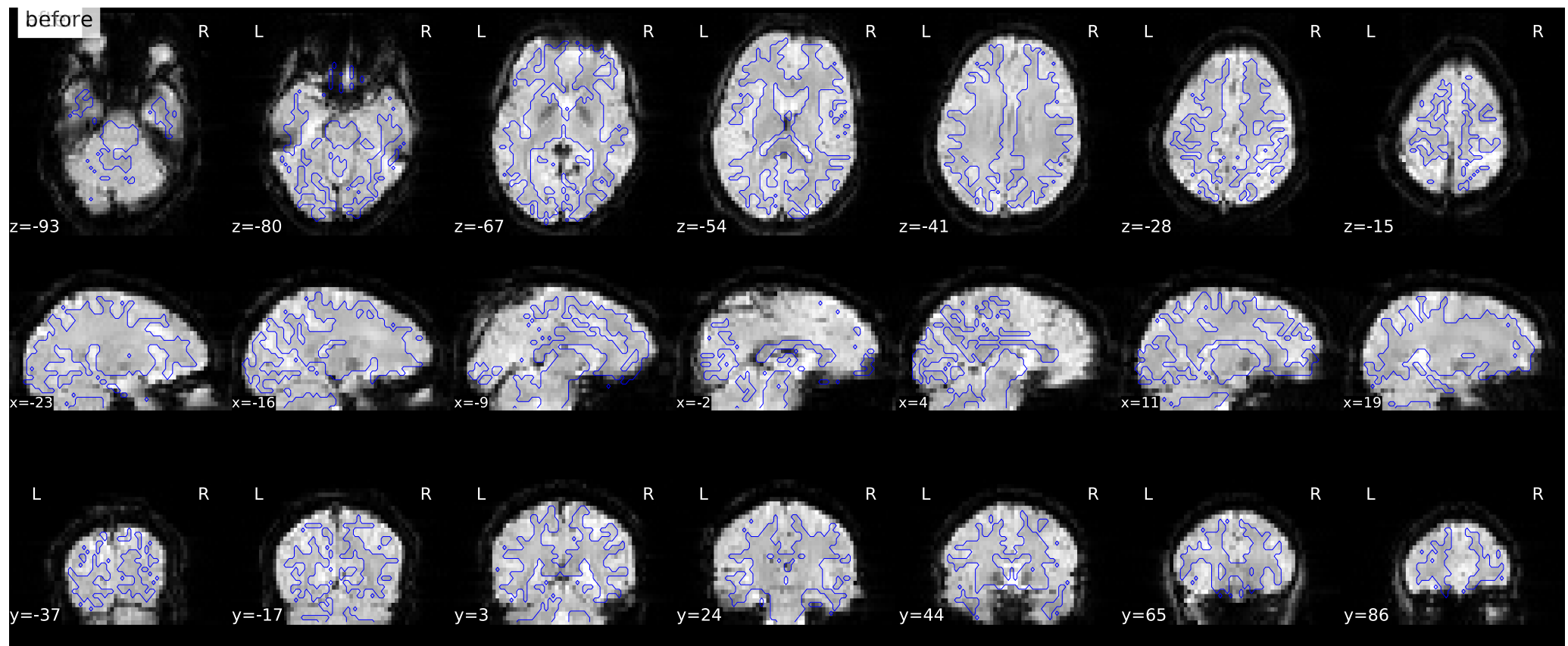
Reports for: task rhymejudgment.

Summary

- Repetition time (TR): 2s
- Phase-encoding (PE) direction: MISSING - Assuming Anterior-Posterior
- Slice timing correction: Not applied
- Susceptibility distortion correction: FLB ("fieldmap-less", SyN-based)
- Registration: FreeSurfer [bbregister](#) (boundary-based registration, BBR) - 6 dof
- Confounds collected: csf, csf_derivative1, csf_derivative1_power2, csf_power2, white_matter, white_matter_derivative1, white_matter_derivative1_power2, white_matter_power2, global_signal, global_signal_derivative1, global_signal_derivative1_power2, global_signal_power2, std_dvars, dvars, framewise_displacement, t_comp_cor_00, t_comp_cor_01, a_comp_cor_00, a_comp_cor_01, a_comp_cor_02, a_comp_cor_03, a_comp_cor_04, a_comp_cor_05, a_comp_cor_06, a_comp_cor_07, a_comp_cor_08, a_comp_cor_09, a_comp_cor_10, a_comp_cor_11, a_comp_cor_12, a_comp_cor_13, a_comp_cor_14, a_comp_cor_15, a_comp_cor_16, a_comp_cor_17, a_comp_cor_18, a_comp_cor_19, a_comp_cor_20, a_comp_cor_21, a_comp_cor_22, a_comp_cor_23, a_comp_cor_24, a_comp_cor_25, a_comp_cor_26, a_comp_cor_27, a_comp_cor_28, a_comp_cor_29, a_comp_cor_30, a_comp_cor_31, a_comp_cor_32, a_comp_cor_33, a_comp_cor_34, a_comp_cor_35, a_comp_cor_36, a_comp_cor_37, a_comp_cor_38, a_comp_cor_39, a_comp_cor_40, a_comp_cor_41, a_comp_cor_42, a_comp_cor_43, a_comp_cor_44, a_comp_cor_45, a_comp_cor_46, a_comp_cor_47, a_comp_cor_48, a_comp_cor_49, a_comp_cor_50, a_comp_cor_51, a_comp_cor_52, a_comp_cor_53, a_comp_cor_54, a_comp_cor_55, a_comp_cor_56, a_comp_cor_57, a_comp_cor_58, a_comp_cor_59, a_comp_cor_60, a_comp_cor_61, a_comp_cor_62, a_comp_cor_63, a_comp_cor_64, a_comp_cor_65, a_comp_cor_66, a_comp_cor_67, a_comp_cor_68, a_comp_cor_69, a_comp_cor_70, a_comp_cor_71, a_comp_cor_72, a_comp_cor_73, a_comp_cor_74, a_comp_cor_75, a_comp_cor_76, a_comp_cor_77, a_comp_cor_78, a_comp_cor_79, a_comp_cor_80, a_comp_cor_81, a_comp_cor_82, a_comp_cor_83, a_comp_cor_84, a_comp_cor_85, a_comp_cor_86, cosine00, cosine01, cosine02, cosine03, trans_x, trans_x_derivative1, trans_x_power2, trans_x_derivative1_power2, trans_y, trans_y_derivative1, trans_y_power2, trans_y_derivative1_power2, trans_z, trans_z_derivative1, trans_z_power2, trans_z_derivative1_power2, rot_x, rot_x_derivative1, rot_x_power2, rot_x_derivative1_power2, rot_y, rot_y_derivative1, rot_y_power2, rot_z, rot_z_derivative1, rot_z_power2, rot_z_derivative1_power2, motion_outlier00, motion_outlier01, motion_outlier02, motion_outlier03, motion_outlier04, motion_outlier05, motion_outlier06, motion_outlier07, motion_outlier08, motion_outlier09, motion_outlier10, aroma_motion_01, aroma_motion_02, aroma_motion_03, aroma_motion_05, aroma_motion_08, aroma_motion_09, aroma_motion_10, aroma_motion_11, aroma_motion_12, aroma_motion_13, aroma_motion_14, aroma_motion_15, aroma_motion_19, aroma_motion_21, aroma_motion_22, aroma_motion_26, aroma_motion_30, aroma_motion_33, aroma_motion_34, aroma_motion_37, aroma_motion_38, aroma_motion_39
- Non-steady-state volumes: 0

Susceptibility distortion correction

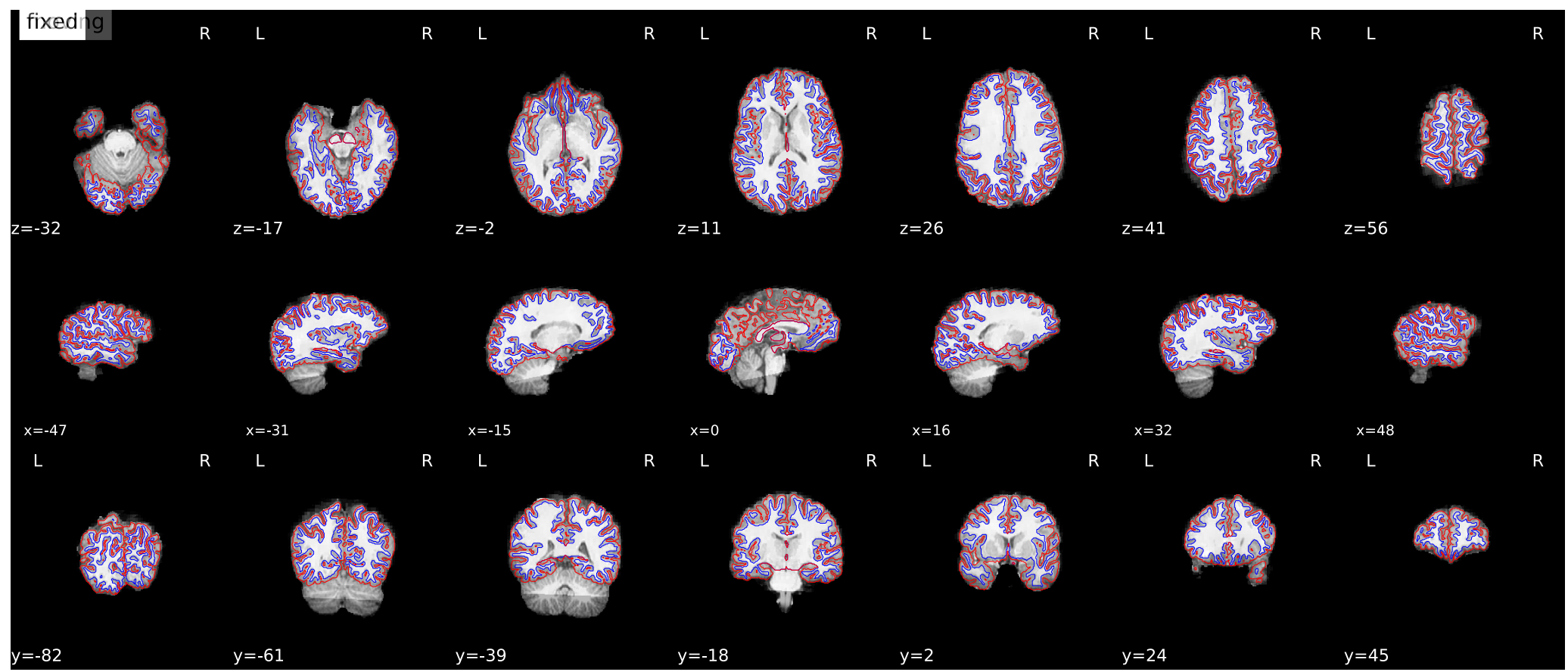
Results of performing susceptibility distortion correction (SDC) on the EPI



Get figure file: [sub-09/figures/sub-09_task-rhymejudgment_desc-sdc_bold.svg](#)

Alignment of functional and anatomical MRI data (surface driven)

`bbregister` was used to generate transformations from EPI-space to T1w-space. Note that Nearest Neighbor interpolation is used in the reportlets in order to highlight potential spin-history and other artifacts, whereas final images are resampled using Lanczos interpolation.



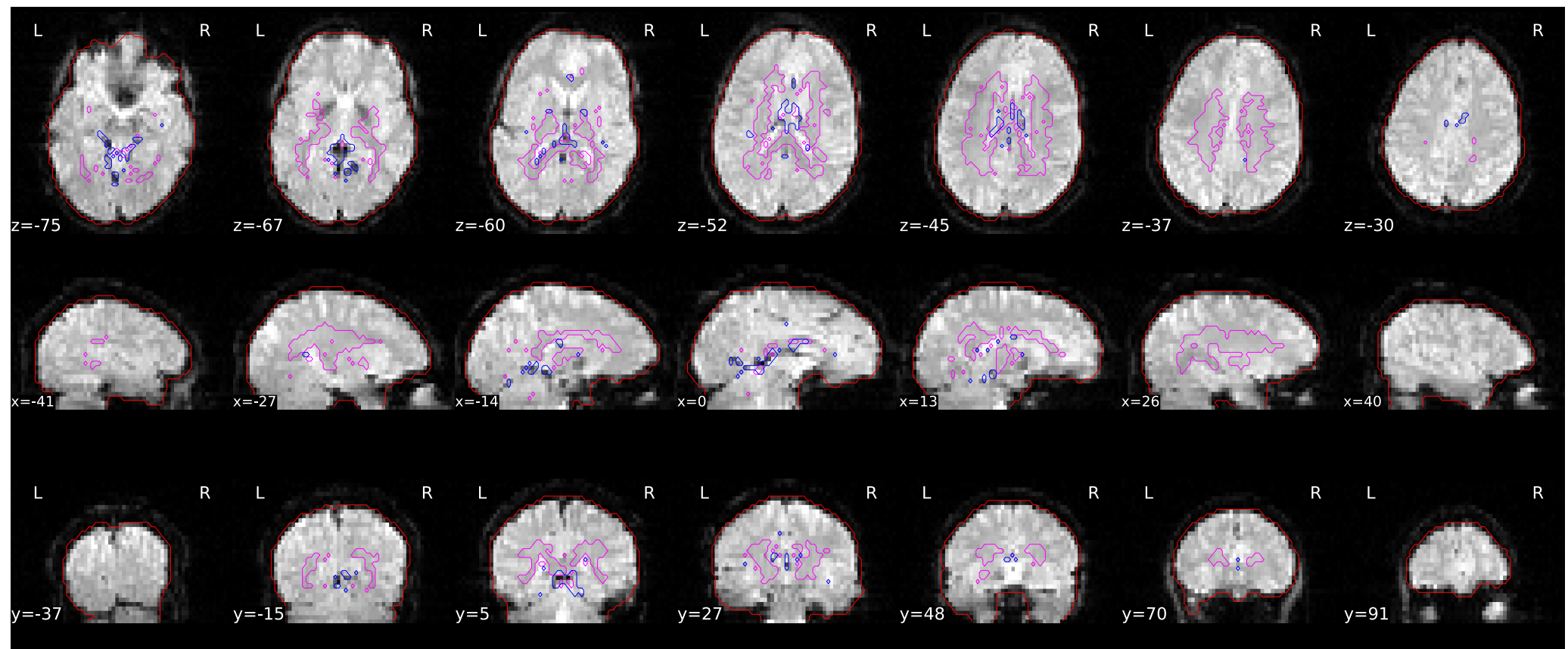
Get figure file: [sub-09/figures/sub-09_task-rhymejudgment_desc-bbregister_bold.svg](#)

Brain mask and (temporal/anatomical) CompCor ROIs

Brain mask calculated on the BOLD signal (red contour), along with the masks used for a/tCompCor.

The aCompCor mask (magenta contour) is a conservative CSF and white-matter mask for extracting physiological and movement confounds.

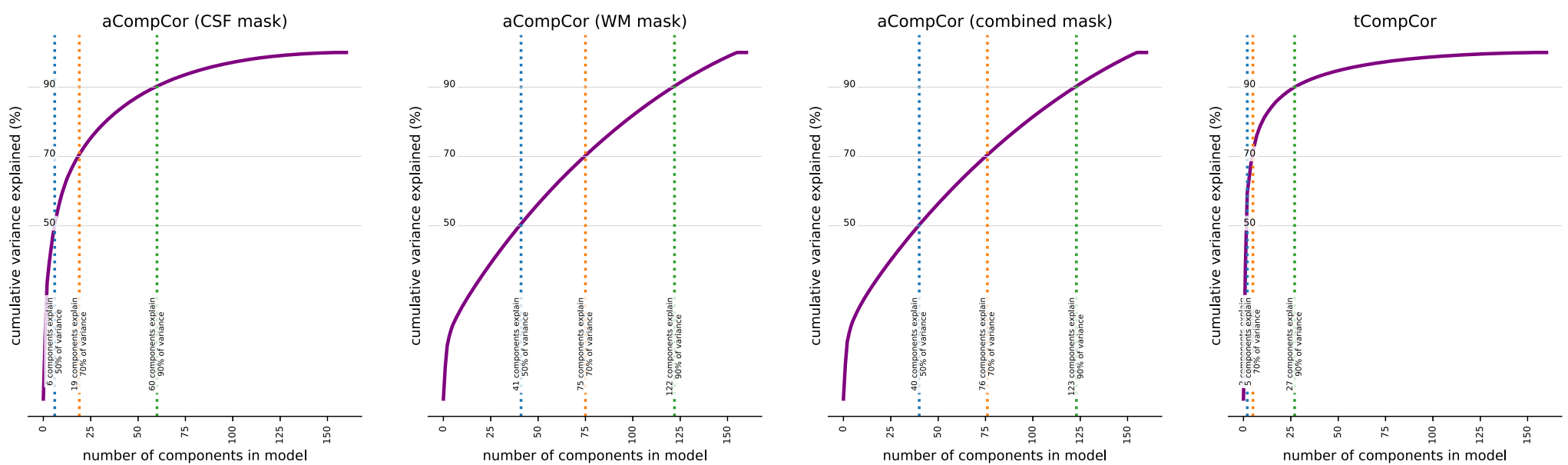
The fCompCor mask (blue contour) contains the top 5% most variable voxels within a heavily-eroded brain-mask.



Get figure file: [sub-09/figures/sub-09_task-rhymejudgment_desc-rois_bold.svg](#)

Variance explained by t/aCompCor components

The cumulative variance explained by the first k components of the $t/aCompCor$ decomposition, plotted for all values of k . The number of components that must be included in the model in order to explain some fraction of variance in the decomposition mask can be used as a feature selection criterion for confound regression.

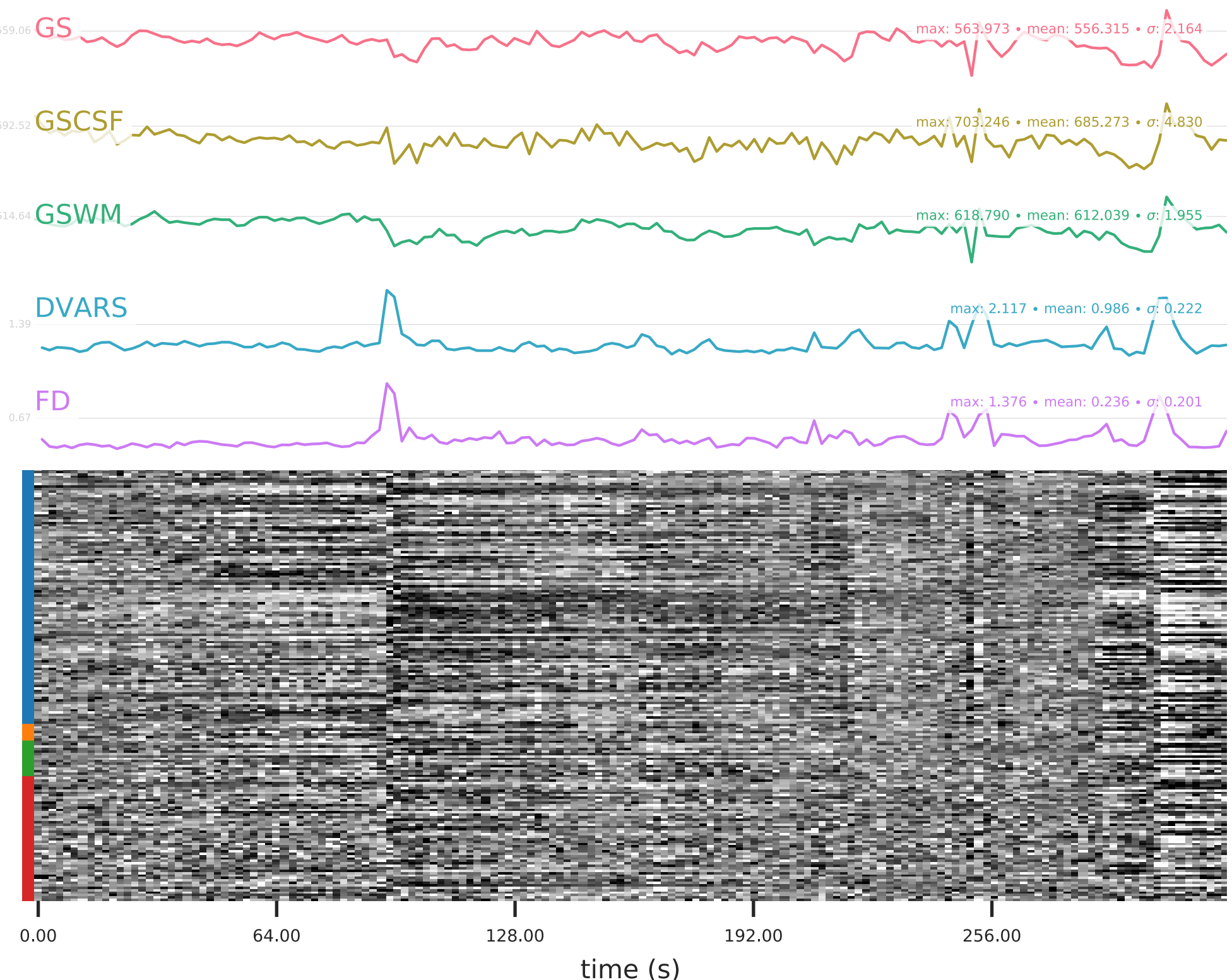


Get figure file: [sub-09/figures/sub-09_task-rhymejudgment_desc-compcorvar_bold.svg](#)

BOLD Summary

Summary statistics are plotted, which may reveal trends or artifacts in the BOLD data. Global signals calculated within the whole-brain (GS), within the white-matter (WM) and within cerebro-spinal fluid (CSF) show the mean BOLD signal in their corresponding masks. DVARS and FD show the standardized DVARS and framewise-displacement measures for each time point.

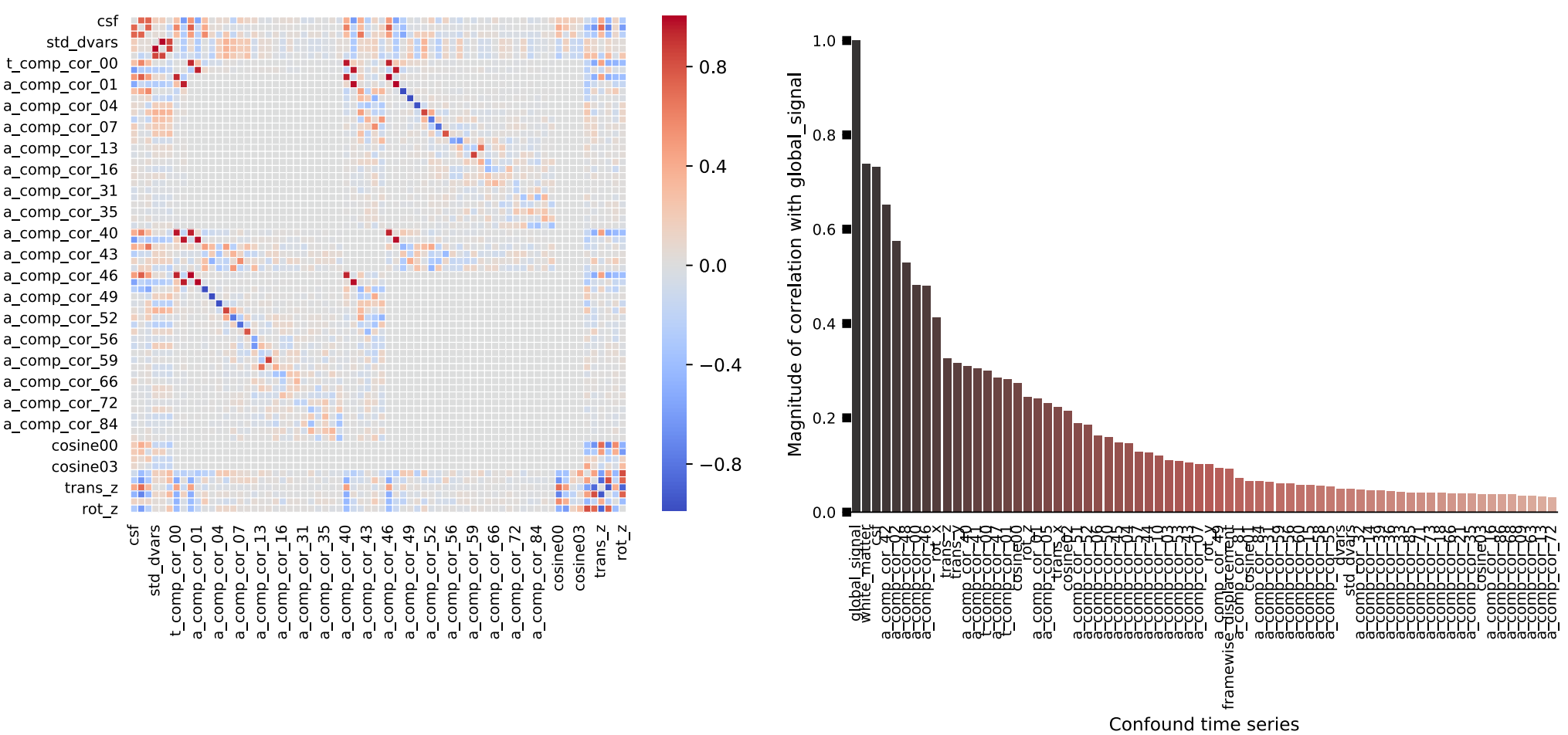
A carpet plot shows the time series for all voxels within the brain mask. Voxels are grouped into cortical (blue), and subcortical (orange) gray matter, cerebellum (green) and white matter and CSF (red), indicated by the color map on the left-hand side.



Get figure file: [sub-09/figures/sub-09_task-rhymejudgment_desc-carpetplot_bold.svg](#)

Correlations among nuisance regressors

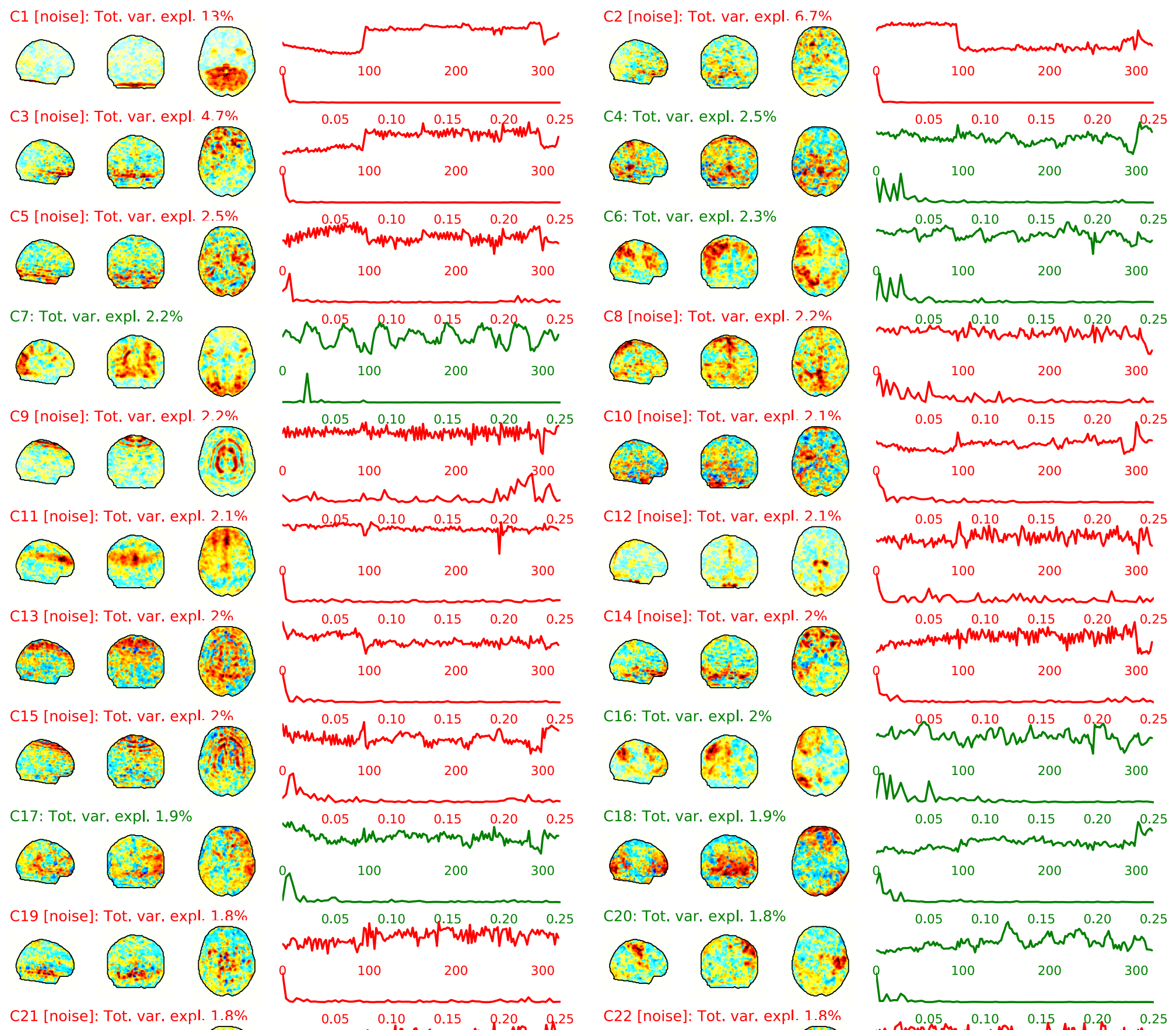
Left: Heatmap summarizing the correlation structure among confound variables. (Cosine bases and PCA-derived CompCor components are inherently orthogonal.) Right: magnitude of the correlation between each confound time series and the mean global signal. Strong correlations might be indicative of partial volume effects and can inform decisions about feature orthogonalization prior to confound regression.

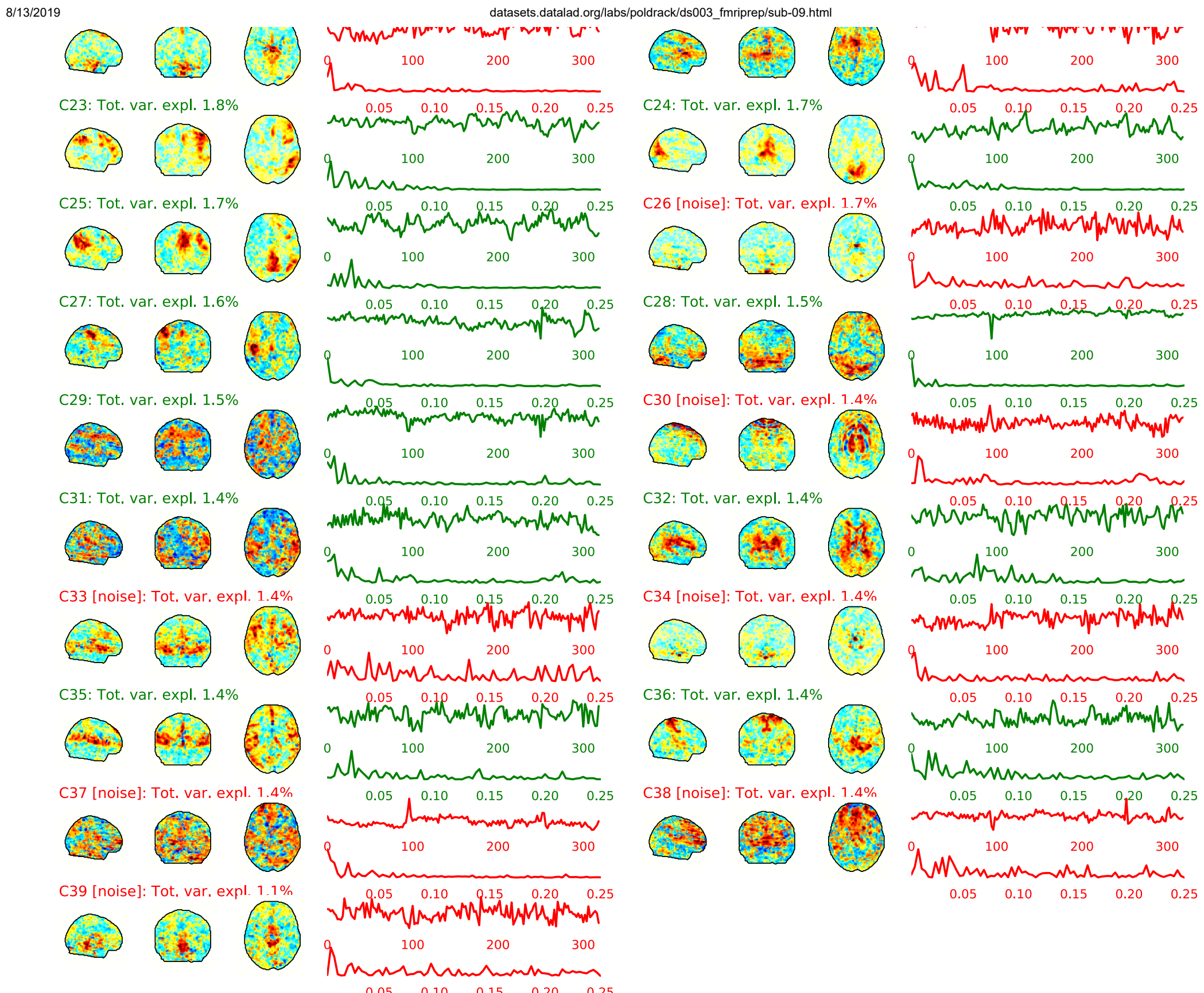


Get figure file: [sub-09/figures/sub-09_task-rhymejudgment_desc-confoundcorr_bold.svg](#)

ICA Components classified by AROMA

Maps created with maximum intensity projection (glass brain) with a black brain outline. Right hand side of each map: time series (top in seconds), frequency spectrum (bottom in Hertz). Components classified as signal are plotted in green; noise components in red.





Get figure file: [sub-09/figures/sub-09_task-rhymejudgment_desc-aroma_bold.svg](#)

About

- fMRIPrep version: 1.4.1
- fMRIPrep command:

```
/usr/local/miniconda/bin/fmriprep /oak/stanford/groups/russpold/data/openfmri/ds000003 /oak/stanford/groups/russpold/data/openfmri/derivatives/ds00003/fmriprep-1.4.1 participant --participant-label 09 -w /work/ --skip_bids_validation --omp-nthreads 8 --nthreads 12 --mem_mb 30000 --output-spaces MNI152NLin2009cAsym:res-2 anat fsnative fsaverage5 --use-syn-sdc --cifti-output --notrack --use-aroma -vv
```
- Date preprocessed: 2019-07-09 10:13:05 -0700

Methods

We kindly ask to report results preprocessed with this tool using the following boilerplate.

[HTML](#) [Markdown](#) [LaTeX](#)

Results included in this manuscript come from preprocessing performed using *fMRIPrep* 1.4.1 (Esteban, Markiewicz, et al. (2018); Esteban, Blair, et al. (2018); RRID:SCR_016216), which is based on *Nipype* 1.2.0 (Gorgolewski et al. (2011); Gorgolewski et al. (2018); RRID:SCR_002502).

Anatomical data preprocessing

The T1-weighted (T1w) image was corrected for intensity non-uniformity (INU) with [N4BiasFieldCorrection](#) (Tustison et al. 2010), distributed with ANTs 2.2.0 (Avants et al. 2008, RRID:SCR_004757), and used as T1w-reference throughout the workflow. The T1w-reference was then skull-stripped with a *Nipype* implementation of the [antsBrainExtraction.sh](#) workflow (from ANTs), using OASIS3oANTs as target template. Brain tissue segmentation of cerebrospinal fluid (CSF), white-matter (WM) and gray-matter (GM) was performed on the brain-extracted T1w using [fast](#) (FSL 5.0.9, RRID:SCR_002823, Zhang, Brady, and Smith 2001). Brain surfaces were reconstructed using [recon-all](#) (FreeSurfer 6.0.1, RRID:SCR_001847, Dale, Fischl, and Sereno 1999), and the brain mask estimated previously was refined with a custom variation of the method to reconcile ANTs-derived and FreeSurfer-derived segmentations of the cortical gray-matter of Mindboggle (RRID:SCR_002438, Klein et al. 2017). Volume-based spatial normalization to two standard spaces (MNI152NLin2009cAsym, MNI152NLin6Asym) was performed through nonlinear registration with [antsRegistration](#) (ANTs 2.2.0), using brain-extracted versions of both T1w reference and the T1w template. The following templates were selected for spatial normalization: *ICBM 152 Nonlinear Asymmetrical template version 2009c* [Fonov et al. (2009), RRID:SCR_008796; TemplateFlow ID: MNI152NLin2009cAsym], *FSL's MNI ICBM 152 non-linear 6th Generation Asymmetric Average Brain Stereotaxic Registration Model* [Evans et al. (2012), RRID:SCR_002823; TemplateFlow ID: MNI152NLin6Asym].

Functional data preprocessing

For each of the 1 BOLD runs found per subject (across all tasks and sessions), the following preprocessing was performed. First, a reference volume and its skull-stripped version were generated using a custom methodology of *fMRIPrep*. A deformation field to correct for susceptibility distortions was estimated based on *fMRIPrep*'s *fieldmap-less* approach. The deformation field is that resulting from co-registering the BOLD reference to the same-subject T1w-reference with its intensity inverted (Wang et al. 2017; Huntenburg 2014). Registration is performed with [antsRegistration](#) (ANTs 2.2.0), and the process regularized by constraining deformation to be nonzero only along the phase-encoding direction, and modulated with an average fieldmap template (Treiber et al. 2016). Based on the estimated susceptibility distortion, an unwarped BOLD reference was calculated for a more accurate co-registration with the anatomical reference. The BOLD reference was then co-registered to the T1w reference using [bbregister](#) (FreeSurfer) which implements boundary-based registration (Greve and Fischl 2009). Co-registration was configured with nine degrees of freedom to account for distortions remaining in the BOLD reference. Head-motion parameters with respect to the BOLD reference (transformation matrices, and six corresponding rotation and translation parameters) are estimated before any spatiotemporal filtering using [mcflirt](#) (FSL 5.0.9, Jenkinson et al. 2002). The BOLD time-series, were resampled to surfaces on the following spaces: *fsnative*, *fsaverage5*, *Grayordinates* files (Glasser et al. 2013), which combine surface-sampled data and volume-sampled data, were also generated. The BOLD time-series (including slice-timing correction when applied) were resampled onto their original, native space by applying a single, composite transform to correct for head-motion and susceptibility distortions. These resampled BOLD time-series will be referred to as *preprocessed BOLD in original space*, or just *preprocessed BOLD*. The BOLD time-series were resampled into several standard spaces, correspondingly generating the following *spatially-normalized, preprocessed BOLD runs*: MNI152NLin2009cAsym, MNI152NLin6Asym. First, a reference volume and its skull-stripped version were generated using a custom methodology of *fMRIPrep*. Automatic removal of motion artifacts using independent component analysis (ICA-AROMA, Pruim et al. 2015) was performed on the *preprocessed BOLD on MNI space* time-series after removal of non-steady state volumes and spatial smoothing with an isotropic, Gaussian kernel of 6mm FWHM (full-width half-maximum). Corresponding “non-aggressively” denoised runs were produced after such smoothing. Additionally, the “aggressive” noise-regressors were collected and placed in the corresponding confounds file. Several confounding time-series were calculated based on the *preprocessed BOLD*: framewise displacement (FD), DVARS and three region-wise global signals. FD and DVARS are calculated for each functional run, both using their implementations in *Nipype* (following the definitions by Power et al. 2014). The three global signals are extracted within the CSF, the WM, and the whole-brain masks. Additionally, a set of physiological regressors were extracted to allow for component-based noise correction (*CompCor*, Behzadi et al. 2007). Principal components are estimated after high-pass filtering the *preprocessed BOLD* time-series (using a discrete cosine filter with 128s cut-off) for the two *CompCor* variants: temporal (tCompCor) and anatomical (aCompCor). tCompCor components are then calculated from the top 5% variable voxels within a mask covering the subcortical regions. This subcortical mask is obtained by heavily eroding the brain mask, which ensures it does not include cortical GM regions. For aCompCor, components are calculated within the intersection of the aforementioned mask and the union of CSF and WM masks calculated in T1w space, after their projection to the native space of each functional run (using the inverse BOLD-to-T1w transformation). Components are also calculated separately within the WM and CSF masks. For each CompCor decomposition, the k components with the largest singular values are retained, such that the retained components' time series are sufficient to explain 50 percent of variance across the nuisance mask (CSF, WM, combined, or temporal). The remaining components are dropped from consideration. The head-motion estimates calculated in the correction step were also placed within the corresponding confounds file. The confound time series derived from head motion estimates and global signals were expanded with the inclusion of temporal derivatives and quadratic terms for each (Satterthwaite et al. 2013). Frames that exceeded a threshold of 0.5 mm FD or 1.5 standardised DVARS were annotated as motion outliers. All resamplings can be performed with a *single interpolation step* by composing all the pertinent transformations (i.e. head-motion transform matrices, susceptibility distortion correction when available, and co-registrations to anatomical and output spaces). Gridded (volumetric) resamplings were performed using [antsApplyTransforms](#) (ANTs), configured with Lanczos interpolation to minimize the smoothing effects of other kernels (Lanczos 1964). Non-gridded (surface) resamplings were performed using [mri_vol2surf](#) (FreeSurfer).

Many internal operations of *fMRIPrep* use *Nilearn* 0.5.2 (Abraham et al. 2014, RRID:SCR_001362), mostly within the functional processing workflow. For more details of the pipeline, see [the section corresponding to workflows in fMRIPrep's documentation](#).

References

Abraham, Alexandre, Fabian Pedregosa, Michael Eickenberg, Philippe Gervais, Andreas Mueller, Jean Kossaifi, Alexandre Gramfort, Bertrand Thirion, and Gael Varoquaux. 2014. "Machine Learning for Neuroimaging with Scikit-Learn." *Frontiers in Neuroinformatics* 8. <https://doi.org/10.3389/fninf.2014.00014>.

Avants, B.B., C.L. Epstein, M. Grossman, and J.C. Gee. 2008. "Symmetric Diffeomorphic Image Registration with Cross-Correlation: Evaluating Automated Labeling of Elderly and Neurodegenerative Brain." *Medical Image Analysis* 12 (1): 26–41. <https://doi.org/10.1016/j.media.2007.06.004>.

Behzadi, Yashar, Khaled Restom, Joy Liau, and Thomas T. Liu. 2007. "A Component Based Noise Correction Method (CompCor) for BOLD and Perfusion Based fMRI." *NeuroImage* 37 (1): 90–101. <https://doi.org/10.1016/j.neuroimage.2007.04.042>.

Dale, Anders M., Bruce Fischl, and Martin I. Sereno. 1999. "Cortical Surface-Based Analysis: I. Segmentation and Surface Reconstruction." *NeuroImage* 9 (2): 179–94. <https://doi.org/10.1006/nimg.1998.0395>.

Esteban, Oscar, Ross Blair, Christopher J. Markiewicz, Shoshana L. Berleant, Craig Moodie, Feilong Ma, Ayse Ilkay Isik, et al. 2018. "FMRIPrep." *Software*. Zenodo. <https://doi.org/10.5281/zenodo.852659>.

Esteban, Oscar, Christopher Markiewicz, Ross W Blair, Craig Moodie, Ayse Ilkay Isik, Asier Erramuzpe Aliaga, James Kent, et al. 2018. "fMRIPrep: A Robust Preprocessing Pipeline for Functional MRI." *Nature Methods*. <https://doi.org/10.1038/s41592-018-0235-4>.

Evans, AC, AL Janke, DL Collins, and S Baillet. 2012. "Brain Templates and Atlases." *NeuroImage* 62 (2): 911–22. <https://doi.org/10.1016/j.neuroimage.2012.01.024>.

Fonov, VS, AC Evans, RC McKinstry, CR Almlí, and DL Collins. 2009. "Unbiased Nonlinear Average Age-Appropriate Brain Templates from Birth to Adulthood." *NeuroImage* 47, Supplement 1: S102. [https://doi.org/10.1016/S1053-8119\(09\)70884-5](https://doi.org/10.1016/S1053-8119(09)70884-5).

Glasser, Matthew F., Stamatios N. Sotiropoulos, J. Anthony Wilson, Timothy S. Coalson, Bruce Fischl, Jesper L. Andersson, Junqian Xu, et al. 2013. "The Minimal Preprocessing Pipelines for the Human Connectome Project." *NeuroImage*, Mapping the connectome, 80: 105–24. <https://doi.org/10.1016/j.neuroimage.2013.04.127>.

Gorgolewski, K., C. D. Burns, C. Madison, D. Clark, Y. O. Halchenko, M. L. Waskom, and S. Ghosh. 2011. "Nipype: A Flexible, Lightweight and Extensible Neuroimaging Data Processing Framework in Python." *Frontiers in Neuroinformatics* 5: 13. <https://doi.org/10.3389/fninf.2011.00013>.

Gorgolewski, Krzysztof J., Oscar Esteban, Christopher J. Markiewicz, Erik Ziegler, David Gage Ellis, Michael Philipp Notter, Dorota Jarecka, et al. 2018. "Nipype." *Software*. Zenodo. <https://doi.org/10.5281/zenodo.596855>.

Greve, Douglas N, and Bruce Fischl. 2009. "Accurate and Robust Brain Image Alignment Using Boundary-Based Registration." *NeuroImage* 48 (1): 63–72. <https://doi.org/10.1016/j.neuroimage.2009.06.060>.

Huntenburg, Julia M. 2014. "Evaluating Nonlinear Coregistration of BOLD EPI and T1w Images." Master's Thesis, Berlin: Freie Universität. <http://hdl.handle.net/11858/00-001M-0000-002B-1CB5-A>.

Jenkinson, Mark, Peter Bannister, Michael Brady, and Stephen Smith. 2002. "Improved Optimization for the Robust and Accurate Linear Registration and Motion Correction of Brain Images." *NeuroImage* 17 (2): 825–41. <https://doi.org/10.1006/nimg.2002.1132>.

Klein, Arno, Satrajit S. Ghosh, Forrest S. Bao, Joachim Giard, Yrjö Häme, Eliezer Stavsky, Noah Lee, et al. 2017. "Mindboggling Morphometry of Human Brains." *PLOS Computational Biology* 13 (2): e1005350. <https://doi.org/10.1371/journal.pcbi.1005350>.

Lanczos, C. 1964. "Evaluation of Noisy Data." *Journal of the Society for Industrial and Applied Mathematics Series B Numerical Analysis* 1 (1): 76–85. <https://doi.org/10.1137/0701007>.

Power, Jonathan D., Anish Mitra, Timothy O. Laumann, Abraham Z. Snyder, Bradley L. Schlaggar, and Steven E. Petersen. 2014. "Methods to Detect, Characterize, and Remove Motion Artifact in Resting State fMRI." *NeuroImage* 84 (Supplement C): 320–41. <https://doi.org/10.1016/j.neuroimage.2013.08.048>.

Pruim, Raimon H. R., Maarten Mennes, Daan van Rooij, Alberto Llera, Jan K. Buitelaar, and Christian F. Beckmann. 2015. "ICA-AROMA: A Robust ICA-Based Strategy for Removing Motion Artifacts from fMRI Data." *NeuroImage* 112 (Supplement C): 267–77. <https://doi.org/10.1016/j.neuroimage.2015.02.064>.

Satterthwaite, Theodore D., Mark A. Elliott, Raphael T. Gerraty, Kosha Ruparel, James Loughead, Monica E. Calkins, Simon B. Eickhoff, et al. 2013. "An improved framework for confound regression and filtering for control of motion artifact in the preprocessing of resting-state functional connectivity data." *NeuroImage* 64 (1): 240–56. <https://doi.org/10.1016/j.neuroimage.2012.08.052>.

Treiber, Jeffrey Mark, Nathan S. White, Tyler Christian Steed, Hauke Bartsch, Dominic Holland, Nikdokht Farid, Carrie R. McDonald, Bob S. Carter, Anders Martin Dale, and Clark C. Chen. 2016. "Characterization and Correction of Geometric Distortions in 814 Diffusion Weighted Images." *PLOS ONE* 11 (3): e0152472. <https://doi.org/10.1371/journal.pone.0152472>.

Tustison, N. J., B. B. Avants, P. A. Cook, Y. Zheng, A. Egan, P. A. Yushkevich, and J. C. Gee. 2010. “N4ITK: Improved N3 Bias Correction.” *IEEE Transactions on Medical Imaging* 29 (6): 1310–20. <https://doi.org/10.1109/TMI.2010.2046908>.

Wang, Sijia, Daniel J. Peterson, J. C. Gatenby, Wenbin Li, Thomas J. Grabowski, and Tara M. Madhyastha. 2017. “Evaluation of Field Map and Nonlinear Registration Methods for Correction of Susceptibility Artifacts in Diffusion MRI.” *Frontiers in Neuroinformatics* 11. <https://doi.org/10.3389/fninf.2017.00017>.

Zhang, Y., M. Brady, and S. Smith. 2001. “Segmentation of Brain MR Images Through a Hidden Markov Random Field Model and the Expectation-Maximization Algorithm.” *IEEE Transactions on Medical Imaging* 20 (1): 45–57. <https://doi.org/10.1109/42.906424>.

Errors

- No errors to report!